JGR Space Physics

RESEARCH ARTICLE
10.1029/2019JA027419

Average Characteristics of Low-Latitude Interhemispheric and *F* Region Dynamo Currents Deduced From the Swarm Satellite Constellation

Hermann Lühr[1], Guram N. Kervalishvili[1], Claudia Stolle[1], Jan Rauberg[1], and Ingo Michaelis[1]

[1]Section 2.3 Geomagnetism, GFZ - German Research Centre for Geosciences, Potsdam, Germany

Key Points:
- Average characteristics of field-aligned and radial currents at low and equatorial latitudes are derived from dual-spacecraft approach
- Low-latitude interhemispheric field-aligned currents show unexpected results during northern winter months
- The *F* region dynamo region above the magnetic equator are found at altitudes depending on longitude, local time, and season

Correspondence to:
H. Lühr,
hluehr@gfz-potsdam.de

Citation:
Lühr, H., Kervalishvili, G. N., Stolle, C., Rauberg, J., & Michaelis, I. (2019). Average characteristics of low-latitude interhemispheric and *F* region dynamo currents deduced from the swarm satellite constellation. *Journal of Geophysical Research: Space Physics*, *124*, 10,631–10,644. https://doi.org/10.1029/2019JA027419

Received 19 SEP 2019
Accepted 23 NOV 2019
Accepted article online 9 DEC 2019
Published online 21 DEC 2019

Abstract Based on magnetic field data from the Swarm satellite constellation advanced estimates of field-aligned and radial currents at middle and low latitudes can be derived. Detailed results have been obtained for low-latitude (14°–35° magnetic latitude) interhemispheric field-aligned currents related to the solar quiet (*Sq*) current system. The continuous data set of five years allows resolving the dependences on local time, season, and longitude. We confirm the known current flow from the southern to the northern hemisphere around June solstice. Unexpected results are obtained for the months following December. Stratospheric sudden warming events are suggested as a reason for that. These phenomena are known to amplify lunar tides and atmospheric planetary waves. Furthermore, we investigated the mean characteristic of the meridional current systems connected to the wind-driven *F* region dynamo above the magnetic equator. Typical features of radially downward currents around noon and upward currents in the evening sector could be confirmed. From a detailed analysis of the connected field-aligned current distribution we deduced that the mean altitude of the dynamo region is higher in the evening than around noon. And it appears also at greater heights in the western hemisphere than in the eastern. Special current configurations are encountered in the longitude range containing the South Atlantic Anomaly. Here summer-like conditions are prevailing through all seasons. This infers that the ionospheric conductivity is significantly enhanced in this region of weak magnetic field strength.

1. Introduction

Ground-based magnetometers regularly observe a diurnal waveform at middle and low latitudes during daytime. This is commonly termed the solar quiet (*Sq*) variation (for reviews, see Campbell, 1989; Yamazaki & Maute, 2017). The *Sq* signal is mainly caused by midlatitude current vortices in the ionosphere. In the northern hemisphere currents are circulating counterclockwise and in the southern clockwise. The intensity of currents varies with solar activity and with season, but tides and planetary waves have also a significant influence. The difference in solar zenith angle between the two hemispheres, in particular during solstices, leads to asymmetries in ionospheric conductivities. All these effects may cause differences in the efficiencies of the wind dynamos at magnetically conjugate points in the two hemispheres (e.g., van Sabben, 1964). Due to the high electrical conductivity along magnetic field lines interhemispheric field-aligned currents (IHFACs) are expected to transfer the excessively generated currents in one hemisphere into the opposite hemisphere and dissipate it there. Based on theoretical considerations field-aligned current densities in the range 1–10 nA/m^2 were predicted (e.g., Maeda, 1974; van Sabben, 1966). Fukushima (1979) proposed a set of IHFACs that should be suitable to remove the differences of the *Sq* systems. According to his model most intense IHFACs connect the *Sq* foci in the two hemispheres (near 35° magnetic latitude (MLat)) around noontime. Here currents should flow from the winter to the summer hemisphere. Around evening somewhat weaker IHFACs, also from winter to summer, are predicted, and in the morning interhemispheric currents should flow in the opposite direct. Observational evidence for IHFACs was first provided by Olsen (1997), based on Magsat data and later by Yamashita and Iyemori (2002) from Ørsted and ground-based data. Due to the limitations of these data sets the full seasonal/local time variations could not be resolved. This was improved by the 10-year CHAMP magnetic field data set. Park et al. (2011) provided the first climatology of IHFACs. For June solstice conditions these authors could confirm in principle the predictions of Fukushima (1979, 1994) except for the evening hours, where they found IHFACs from the summer to the

winter hemisphere. But for the months around December solstice they reported a rather complex pattern of IHFACs, not confirming the expectations. There were also attempts to estimate IHFAC from ground-based magnetic field measurements. For example, Bolaji et al. (2012) and Owolabi et al. (2018) tried to determine IHFAC variations over Africa from readings of the MAGDAS magnetometer network. Shinbori et al. (2017) studied the long-term variation of the *Sq* system in the East Asian and Pacific region. As a side aspect, they could also provide a qualitative estimate of diurnal IHFAC variation over Guam. Their curves are in good agreement with the results of Park et al. (2011), but at odd with the predictions of Fukushima (1979) for the evening hours.

For deriving interhemispheric currents from a polar orbiting satellite like CHAMP Park et al. (2011) assumed that FACs are stationarity in time and organization in elongated FAC sheets perpendicular to the orbit, which may add uncertainties to their results. Here the Swarm satellite constellation can help to provide more reliable IHFAC values. By applying the dual-spacecraft (dual-SC) approach to magnetic field measurements of the two spacecraft Swarm A and C, flying side-by-side, less constrained field-aligned current estimates can be achieved (Ritter et al., 2013). Based on these dual-SC Swarm current estimates Lühr et al. (2015) performed an initial study of IHFACs. But due to the limited amount of data at that time they could only investigate northern summer and fall conditions. Their results confirmed well the findings of Park et al. (2011). Recently, Fathy et al. (2019) performed an extensive IHFAC study based on four years of Swarm dual-SC data. They considered for their analysis the 10 quietest days of a month and confirmed in general earlier findings. One of their observations is that the direction of IHFACs commonly switch sign around 35° magnetic latitude in both hemispheres, but they do not provide any suggestion for the processes that may be responsible for it.

Another topic of interest for the current study is the wind-driven *F* region dynamo. This concept of a dynamo in the topside ionosphere over the magnetic equator was introduced by Rishbeth (1971). He predicted radially upward currents in the evening sector where strong eastward winds are prevailing. The first evidence for related currents came from Magsat observations (e.g., Maeda et al., 1982; Olsen, 1997; Takeda & Maeda, 1983). Later, Lühr and Maus (2006) showed, based on CHAMP observations, that besides the upward currents in the evening sector there appear downward currents around noontime. This was later confirmed by more comprehensive studies of the *F* region dynamo by Park, Lühr, and Min (2010) and Park, Lühr, Fejer, and Min (2010) including the dependence on season, longitude, and solar activity. Again, a caveat of these early studies is that they are based on single satellite magnetic field data. This required important assumptions. Any deflection of the eastward magnetic component during crossing of the magnetic equator was interpreted as caused by either IHFACs or *F* region dynamo currents, deduced from the symmetric or antisymmetric variations, respectively. Here again, the readings from the lower pair, Swarm A and C, are used in the dedicated approach to estimate the radial current components.

The aim of this study is to find out the true average characteristics of IHFACs and *F* region dynamo currents by resolving the details of the various dependences. The analysis is based on five years of 1-Hz Swarm magnetic field data, making use of the advanced dual-SC current estimates. This data set allows resolving seasonal/local time variations and shows longitude dependences. More detailed results of the investigated current systems are expected.

In the subsequent sections we will first introduce the data set and the analysis approach for deriving the radial and field-aligned current components. It is follows by a presentation of observations, first of low-latitude IHFACs and then of radial current estimates at equatorial latitudes. Subsequently, we discuss the average properties of these current components and compare them with earlier publications. In the end we summarize the findings and draw conclusions.

2. Data and Processing Approach

On 22 November 2013 European Space Agency's (ESA's) Earth Observation (EO) mission Swarm was launched into a near-polar orbit. After the commissioning phase the final constellation of the three-satellite mission was achieved on 17 April 2014. The two satellites Swarm A and C (at about 460-km altitude) fly side-by-side, separated by 1.4° in longitude. Swarm B is cruising somewhat higher at 510 km. All satellites are equipped with an identical set of six instruments (see Friis-Christensen et al., 2008). Here we make use of the magnetic field vector data, sampled by the vector fluxgate magnetometer. The vector data are

calibrated against the Absolute Scalar Magnetometer, a helium vapor instrument. This procedure ensures high accuracy of the magnetic field data from all three spacecraft.

The vertical current density estimates are derived by applying Ampère's ring integral:

$$j = \frac{1}{\mu_0 A} \oint B \, dl \tag{1}$$

where A is the area encircled by the contour, B is the magnetic field caused by the current, dl is the line element along the integration path, and μ_0 is the permeability of free space. In practice we use four readings forming the corners of a quadrangle. Details of the current analysis have been described earlier by Ritter et al. (2013), and here we follow directly the approach presented by Lühr et al. (2020).

The primary product of integrating the magnetic field along the border of the horizontal quad formed by the readings from the two Swarm spacecraft is the mean value of the radial current density passing the encircled area. Since Swarm A and C are separated by about 150 km at low latitudes, we only can resolve large current structures with horizontal scales larger than 150 km. For that reason, the magnetic field data are filtered, in order to suppress small fluctuations, before computing the mean current density. In the following we will refer to this quantity as ionospheric radial current (IRC).

In the topside ionosphere the electrical conductivity along geomagnetic field lines is several orders of magnitudes larger than the transverse conductivity. For that reason, the radial current component can commonly be interpreted as caused by field-aligned currents (FACs). We partly follow that approach and estimate FAC density by dividing IRC by the negative sine of the magnetic inclination angle. FAC estimates, however, become unreliable for too small inclinations. IRCs are therefore not mapped onto the field direction near the magnetic equator at inclinations smaller than 30°. Within that low-latitudinal range only the IRC results are interpreted. Both quantities, the dual-SC IRC and FAC, are routinely processed by ESA EO as Swarm Level-2 product FAC_TMS_2F, and they are freely accessible to all users via ftp://swarm-diss.eo.esa.int/Level2daily/Latest_baselines/FAC/TMS/Sat_AC/.

3. Low-Latitude Field-Aligned Currents

As described above, any difference in dynamo efficiency between magnetically conjugate points in the ionosphere will drive IHFACs. For sensing these rather weak currents we make use of the dual-SC estimates. These are available since 17 April 2014, and we take advantage of the subsequent five-year data set. This is the declining phase of solar cycle 24, lasting from its peak with $F_{10.7}$ values reaching beyond 150 sfu down to the present minimum with $F_{10.7}$ ranging around 70 sfu. The study by Park et al. (2011) has shown that the solar flux level has little influence on the distribution of IHFACs. Therefore, no data selection is applied. A period of five years is just the time Swarm satellites need to provide the even coverage of local times during all seasons.

Figure 1 shows as an example one satellite pass of middle- to low-latitude FACs during noontime on 15 May 2014. Positive values represent currents from the southern to the northern hemisphere. No FACs are shown for satellite positions within ±15° MLat because of the low inclination (<30°), as explained above in section 2 . On this day the mean current densities are quite high. Amplitudes can vary considerably from day to day. The large-scale structures in the two successively sampled hemispheres are quite similar, showing FACs that flow out of the southern (winter) into the northern (summer) hemisphere, as expected for this local time. Smaller features do not match so well. This could be due to temporal/spatial differences of the E region dynamos between magnetically conjugate locations during the 20-min passage.

3.1. Average Properties of IHFAC

The focus of this study is to find out the mean currents that are required to shorten out the potential differences between the two hemispheres. For that reason, we consider only the net FAC flowing between conjugate locations. In practice, we took the mean value of the FAC readings at conjugate latitudes in the two hemispheres as the IHFAC value. A FAC measured by the satellites is mapped down along field line, and for further analysis its coordinates at E region altitude are assigned to the current density value. In this way, altitude changes of the satellites are taken into account for localizing the source region. Here we consider IHFAC averages connected to magnetic latitudes in the E region from 20° to 35° MLat in both

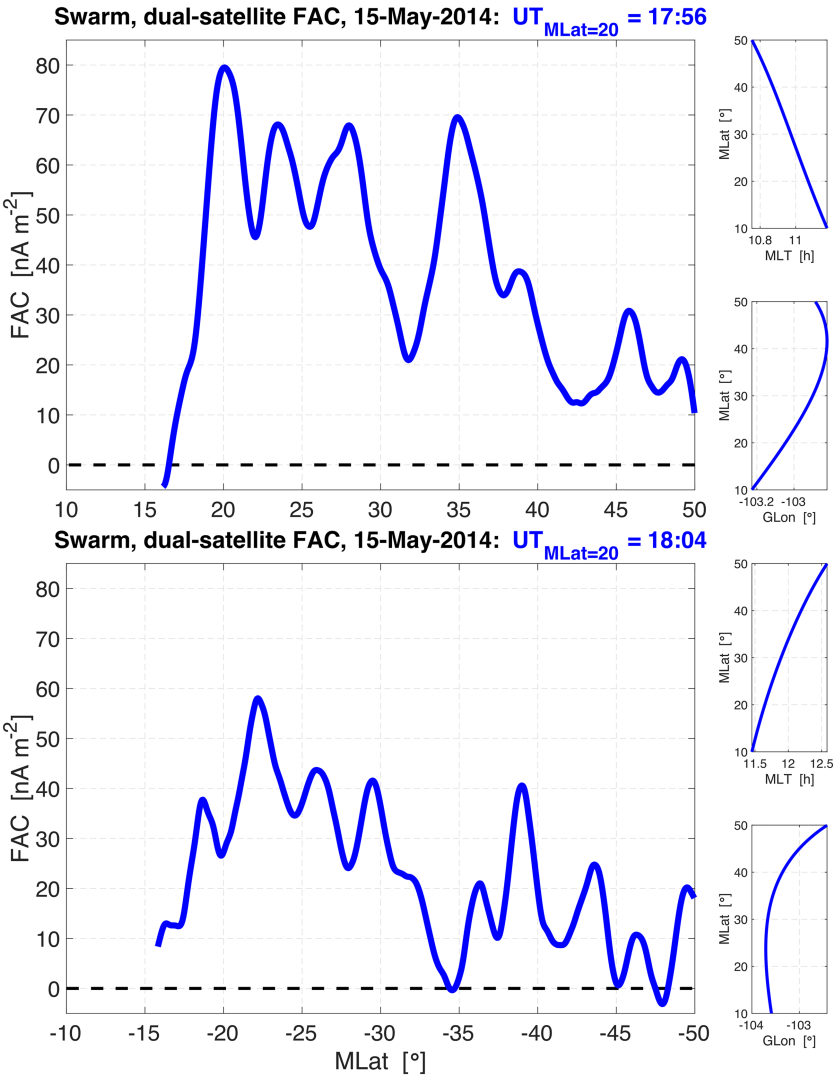

Figure 1. Examples of middle-, low-latitude noontime field-aligned currents along quasi-conjugate profiles in the two hemispheres. The positive values reflect interhemispheric currents from south to north.

hemispheres. The low-latitude boundary is dictated by the truncation of FAC estimates at inclination angles less than 30°. Earlier studies, for example, Fathy et al. (2019), have shown that FACs with opposite direction often are found at latitudes beyond 35° MLat. In order to avoid contamination by them we did not take IHFACs poleward of 35° MLat into account in the averages.

Figure 2 shows the diurnal variation of the mean IHFAC density within 20°–35° MLat averaged over all years and all longitudes but separately for the three Lloyd seasons. Each season comprises four months centered around June solstice, December solstice, or the combined equinox seasons, as indicated in the headings of the frames. For the June solstice season we obtain the classical picture of IHFACs. Peak current densities of 10 nA/m^2 flowing from the southern to the northern hemisphere are found around noon. Somewhat weaker IHFACs appear during morning and evening hours. Current features at night are not further discussed in this study.

As expected for equinox conditions, IHFAC amplitudes are smaller than those around June. During spring and fall the difference in *Sq* current systems in the two hemispheres should be smallest. Overall, the equinox curve shows certain similarity with that for June solstice.

Quite surprising is the curve for December solstice conditions. Theoretically, a mirror image of the June curve would have been expected. But actually, only very small mean IHFAC densities with polarity

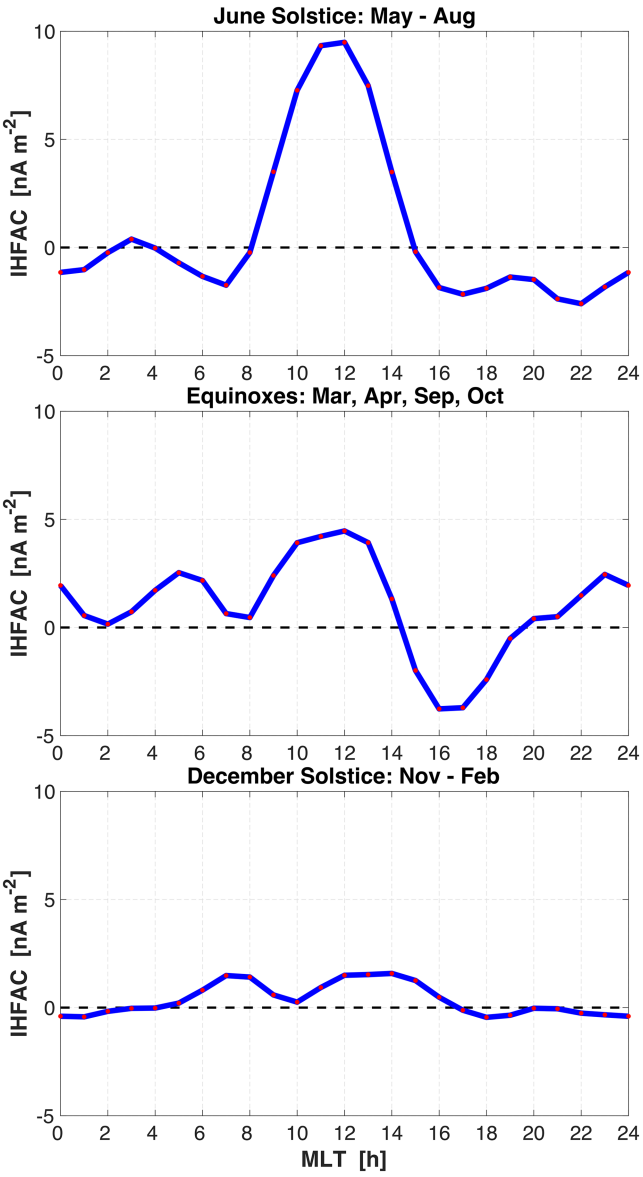

Figure 2. Average local time dependence of the low-latitude interhemispheric field-aligned currents separately for the three Lloyd seasons. Positive values represent currents flowing northward.

opposite to expectation emerge. This may suggest almost equally strong *Sq* systems in the two hemispheres, or *Sq* systems, which are highly variable both in time and longitude, such that the mean averages close to zero. In subsequent sections we will look deeper into these issues.

3.2. Longitudinal Variation of IHFACs

The large number of Swarm orbits (about 28,000) during the five years considered allows us to resolve the diurnal variations at all the longitudes. With that we obtain a more detailed insight into the IHFACs. Figure 3 shows the IHFAC intensity distributions in magnetic local time (MLT) versus geographic longitude (GLon) frames. During the months around June solstice (top panel) the diurnal variation changes only little with longitude. We obtain a well-stratified picture with strong northward currents around noon and southward in the morning and evening. The local time of peak current density varies slightly between 11 and 13 MLT. Peak currents are attained progressively later, the further north the magnetic equator is located. The noontime current is weakest at longitudes between 300°E and 330°E. This coincides with the longitude sector of the South Atlantic Anomaly (SAA). The four current density peaks near noon, at longitudes around 60°E, 150°E, 240°E, and less prominent at 350°E, had earlier been noticed by Park et al. (2011). They related this wave number-4 longitudinal feature to the well-known diurnal nonmigrating solar tide DE3 that is driven from below. The mean IHFAC distribution during the equinoxes resembles in many respects the June solstice situation but at lower current densities. For example, the noontime current density minimum in the SAA sector and wave number 4 current peaks match well the June distribution.

A quite different picture of IHFAC distribution emerges for the northern winter season (Figure 3, bottom). The mean current densities show significant variation with longitude. At hardly any longitude sector a diurnal IHFAC distribution is observed as predicted by the Fukushima (1979) model. Just the sector 180°–240° GLon comes closest to it, northward IHFAC in the morning and southward IHFACs at noon and evening hours. But this is probably just a random coincidence caused by the interaction between several drivers. A more realistic explanation for the observed particular longitudinal variations is the effect of atmospheric tides on the *Sq* current system. An obvious candidate for that is the semidiurnal westward propagating solar tide SW1. For guiding the eyes, a dashed line is added in the plot marking the possible phase front of the wave crest and a solid line for the wave trough. Regardless of the current system modulation by tidal drivers, we do not observe the net dominant current flow from the winter into the summer hemisphere, as found around June solstice.

4. Equatorial *F* Region Dynamo Currents

Close to the magnetic equator the derived radial current components can be used for studying the characteristics of the wind-driven *F* region dynamo. Figure 4 shows estimates of IRC from two passes over the magnetic equator. The example in the top frame, 1 May 2014, is from noontime and the one below, 1 July 2014, from evening hours. In the top frame we observe, besides some significant oscillations, a mean trend of upward currents in the southern hemisphere changing to downward currents in the northern. Large-scale mean current densities are quite small, ranging around 10 nA/m^2. The radial currents from evening hours, bottom frame, are flowing upward at all latitudes. Current density peaks around the magnetic equator, but the amplitude stays below 10 nA/m^2. As expected, the current distribution varies significantly from day to day. Therefore, it is difficult to draw firm conclusions from these single-pass current profiles.

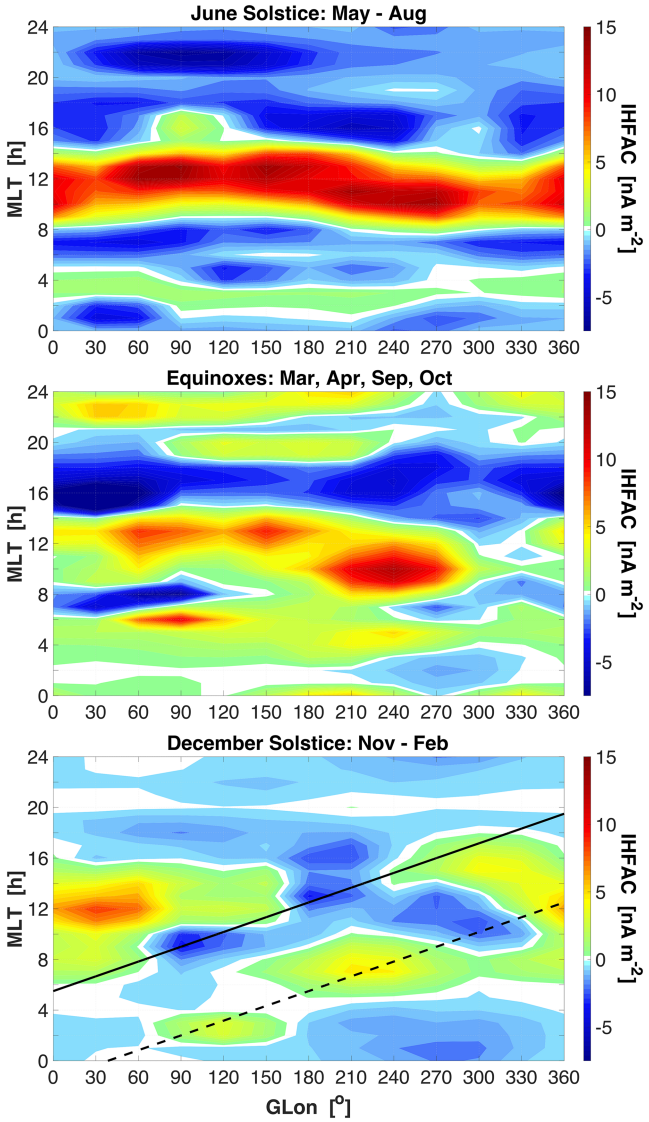

Figure 3. Mean local time versus longitude distribution of interhemispheric field-aligned currents separately for the three Lloyd seasons. The dashed and solid lines in the bottom frame mark the crest and trough of a semidiurnal SW1 tide.

Figure 5 shows the mean diurnal variation of radial currents averaged over the five years, again separately for the three Lloyd seasons. At latitudes beyond ±5° MLat oppositely directed IRCs are dominating. These are indications for IHFACs, and they are particularly prominent during June solstice months around noon. Their diurnal variation is consistent with the mean IHFAC curves in Figure 2. Of more interest here is the IRC distribution within the ±5° MLat band. Around noontime we find at all seasons downward currents above the magnetic equator. These are weakest around June and strongest at equinox months. Peak current densities occur right around noon during June season and about 1 hr later during the other seasons of the year.

Around evening hours radially outward flowing currents are observed during all seasons. Current densities are commonly higher than at noontime. Interestingly, they do not peak right at the equator but bifurcated IRC structures are found in all cases. Here again, the peak radial currents occur around June about 1 hr earlier than during the other seasons.

For better understanding the equatorial current observations we should have a look at the full current system comprising the *F* region dynamo. Figure 6 illustrates schematically the complete wind-driven meridional current systems for both local time sectors around noon and at dusktime. Thermospheric zonal wind over the equator is directed westward during prenoon and daytime hours and turns eastward around 15 MLT (e.g., Lühr et al., 2012). The vertical currents in the dynamo region are diverted into field-aligned meridional current systems in the two hemispheres for current closed. Depending on the orbital height, the satellites will sample different parts of the current system. In the case of a relatively large altitude it will cross besides the vertical current the upper pair of FAC legs. In the case of a too low orbit the satellite may miss the vertical current in the dynamo region and cross only the lower pair of FAC legs. According to these considerations, the two observed upward current peaks on both sides of the magnetic equator around evening hours (see Figure 5) indicate that Swarm A and C passed on average below the *F* region dynamo in that time sector.

4.1. Longitude Variation of Noontime *F* Region Dynamo Currents

So far, we have seen only the mean radial currents at low latitudes, averaged over all longitudes. More details may be revealed when resolving the longitudinal distribution. Figure 7 shows the IRC density in magnetic latitude versus geographic longitude frames separately for the three seasons. Dashed lines mark again the ±5° MLat, the latitude range where the *F* region dynamo dominates the electrodynamics. Current distributions shown here are averages over the 4 hr around noontime when the downward currents peak. For the months around June these are the local time hours 10–14 MLT and for the other two seasons the hours 11–15 MLT.

At latitudes poleward of the dashed lines clear signatures of the interhemispheric currents are visible (oppositely directed IRC). They repeat main features of the noontime IHFACs shown in Figure 3. For June solstice months we find at low latitudes a rather homogeneous longitudinal distribution with some weak areas around the SAA. During equinoxes the June direction of IHFACs is still observed except for the SAA region (around 300° GLon) where the currents flow southward. Also, in this presentation we confirm the unexpected low-latitude current distribution for the December months. Overall, current densities are here very low for a solstice season, and the expected direction for that season, upward in the north and downward in the south, is only partly found in the longitude sector 180°–270° GLon. Possible reasons for that will be discussed in section 5.

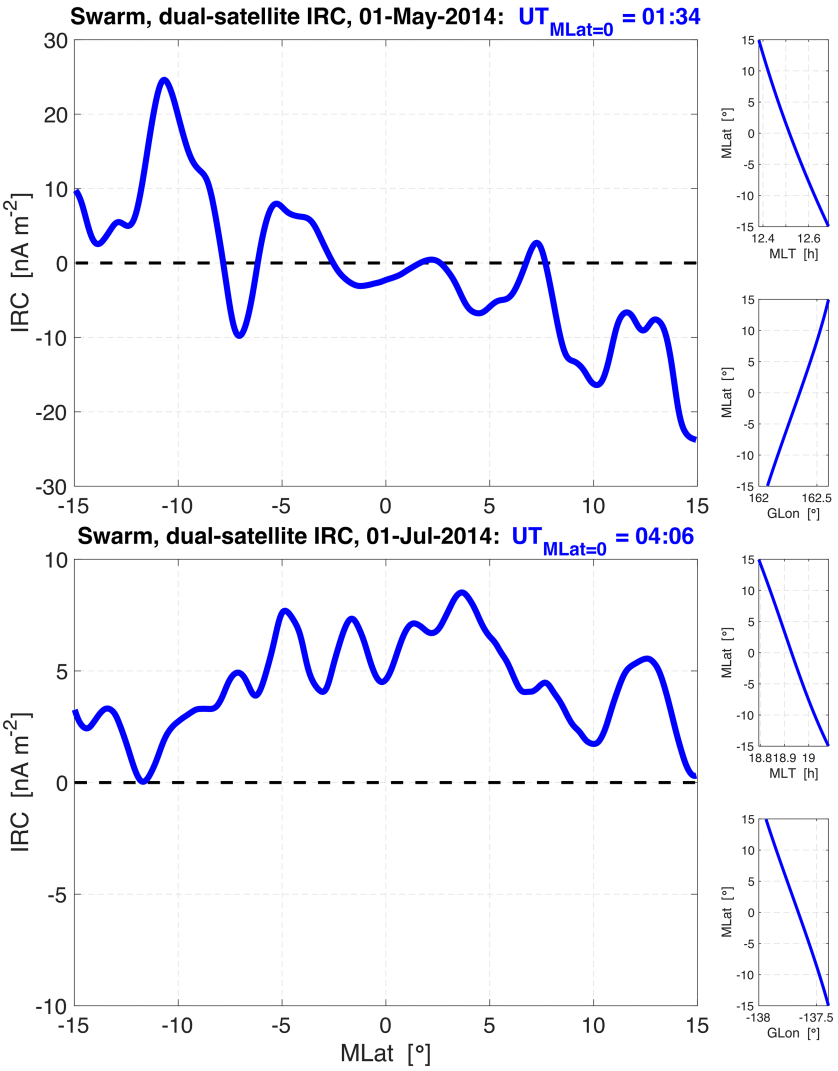

Figure 4. Examples of low-latitude radial currents, (top) around noontime and (bottom) in the evening sector. Positive values represent upward currents.

More interesting here are the current features close to the magnetic equator. Around June season the downward current is very weak (1–2 nA/m^2). A faint enhancement of it at the equator is observed in the eastern hemisphere (0°–180° GLon). The upward IRCs in the southern hemisphere reach almost latitudes up to the magnetic equator. We interpret this as a constructive overlap of the upward IHFAC in the southern hemisphere with the upper FAC leg of the meridional system (see Figure 6). In the northern hemisphere these two current components flow in opposite directions and almost compensate each other. This infers that Swarm passed the equator primarily at the very top of the dynamo region.

More prominent downward IRCs are recorded during equinoxes. But also here current densities are higher in the eastern hemisphere, as it is observed around December solstice months. We interpret it in terms of the higher altitude of the *F* region dynamo in the eastern hemisphere during all seasons and therefore at a more favorable location for crossing of the current system by Swarm. The assumption of a lower dynamo region in the western hemisphere is also supported by the near-equator intrusion of the upward IRC around 300° GLon during equinoxes. Here the same arguments hold for a constructive overlap of upward IHFACs in the northern hemisphere with the upper FAC leg of the meridional system.

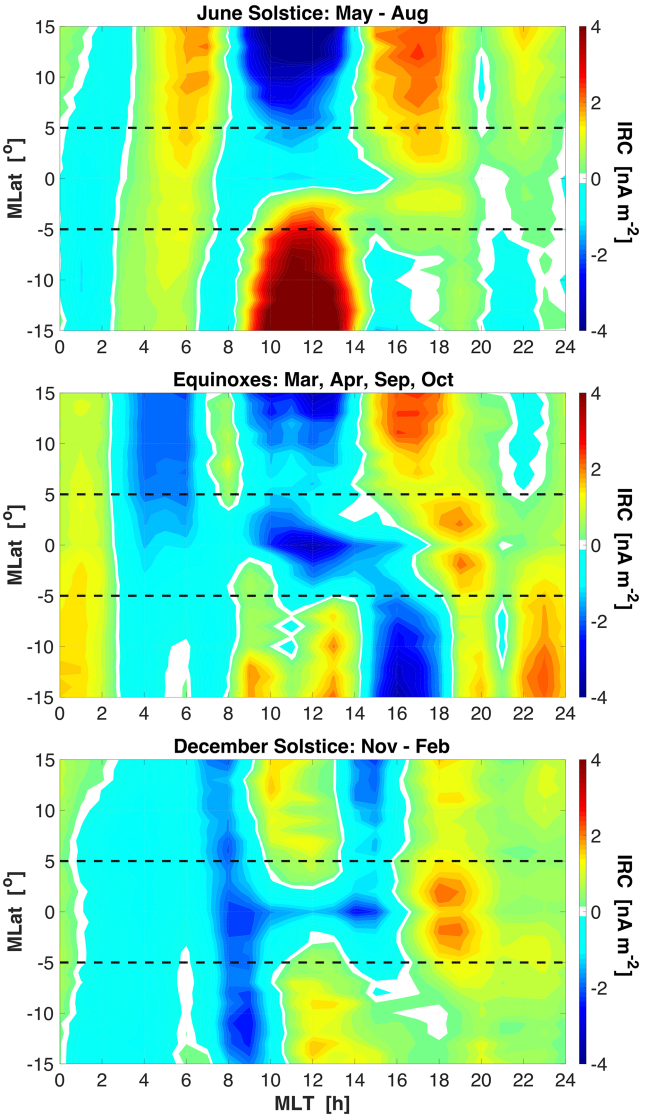

Figure 5. Mean local time versus magnetic latitude distribution of radial *F* region currents separately for the three Lloyd seasons. Positive values represent upward flowing currents. The horizontal dashed lines can be regarded as demarcation lines between IHFACs and *F* region dynamo driven currents.

4.2. Longitude Variation of Dusktime *F* Region Dynamo Currents

In the same format as for the noontime *F* region currents, Figure 8 presents the longitude distribution of the dynamo currents within the dusktime. Currents shown here are averages of the three local time hours where we observed in Figure 5 the highest IRC density over the magnetic equator. These are the hours 17–19 MLT for June conditions and 18–20 MLT for the other two seasons. Also here, the dashed lines at ±5° MLat delineate quite well the two low-latitude current systems. At equatorial latitudes the largest upward current densities are found around 240° GLon during all seasons. This is contrasting the weaker noontime currents in this sector. In the eastern hemisphere (0°–180° GLon) we find a bifurcation of outward IRCs (best visible at equinoxes). According to our cartoon in Figure 6 this suggests for the duskside that Swarm passed the meridional current system below the dynamo region, crossing just the lower pair of upward FAC legs. When following these arguments all this implies, the *F* region dynamo region is located at higher altitudes during the evening hours than around noontime, and it is found systematically lower in both local time sectors in the western than in the eastern hemisphere.

Just for completeness it may be noted that the special effect of the SAA on IHFACs is also in Figure 8 prominently visible in the longitude sector 300°–330° GLon.

5. Discussion

Mean characteristics of equatorial and low-latitude *F* region currents have been derived from Swarm magnetic field measurements. The lower pair, Swarm A and C, allows for deriving reliable field-aligned and radial current estimates by means of the dual-spacecraft approach. In an initial study Lühr et al. (2015) made use of the first half-year of Swarm constellation data (April through October 2014) for studying the low-latitude *F* region currents. The new analysis, considering five years of Swarm measurements, confirms the early results. Both their mean diurnal variation and the longitudinal distribution of IHFAC agree well with our results shown in Figures 2 and 3 for June solstice conditions. As mentioned earlier, the equinox IHFAC distribution is quite similar to that of June solstice. Just by good fortune, the study of Lühr et al. (2015), making use of the northern summer and fall months, revealed in principle the classical IHFAC features, as expected by theoretical considerations (e.g., Fukushima, 1979) for June solstice conditions.

A totally different result is obtained for northern winter conditions. During that season the observed IHFACs agree in no way with the predictions. On global average there is around noontime practically no net field-aligned current flowing from the winter into the summer hemisphere. This is a surprising result. Already Park et al. (2011) reported an unexpected IHFAC distribution around December solstice, derived from CHAMP magnetic field recordings. Their Figure 2d shows also an almost vanishing mean current flow between the hemispheres. One reason for that is the particular longitudinal pattern of IHFAC density during this season. Main current features in their Figures 5b and 6d are confirmed by our Figure 3d. Please note that Park et al. (2011) used a different color scale. In their case red color represents IHFACs from the northern to the southern hemisphere. These authors suggest that atmospheric tidal winds are responsible for the longitudinal patterns. However, tidal modulation cannot explain the lack of net current flow from the winter to the summer hemisphere around noon.

In the following we may have a look at the *Sq* current systems in the two hemispheres during the different seasons. Chulliat et al. (2016) presented a comprehensive analysis of the *Sq* current system on a

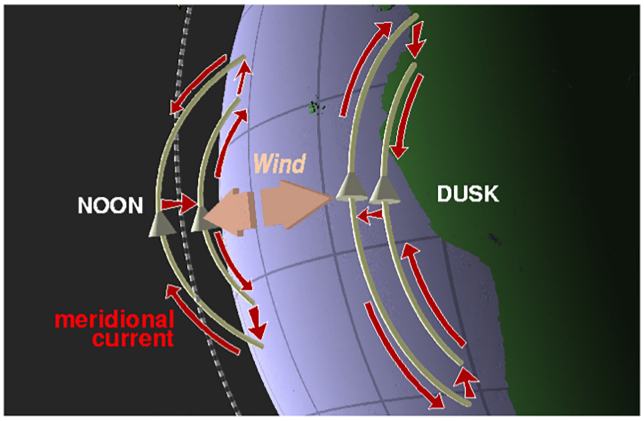

Figure 6. Schematic illustration of the *F* region dynamo over the dip equator driven by thermospheric winds. Related meridional current systems are set up both in the noon and dusk sectors (modified after Lühr & Maus, 2006, Figure 2).

global scale, based on ground-based and Swarm magnetic field observations. In their Figure 12 they show the universal time (UT) dependence of the derived peak *Sq* current function (representing the total current in the dayside vortex) separately for the four seasons and the two hemispheres. In the southern hemisphere current functions show rather flat longitudinal profiles (somewhat modulated by tidal activity; e.g., DE2, DE3) for all seasons. Just the mean values vary from season to season. In the northern hemisphere the stream functions of spring, summer, and fall follow a common longitudinal variation (less affected by tides). However, the winter curve is quite different. Lowest current intensities are reported for 07–10 UT (corresponding to noontime in the longitude sector 30°–75° GLon) and highest for 16–17 UT (noon at 285°–300° GLon). The ratio of these extrema is as large as 1 to 3. And interestingly, the longitudinal average of the total *Sq* current is almost the same in the two hemispheres during December solstice season. This may well explain the observed lack of net IHFACs from winter to summer during that season. However, when comparing the longitude sector of weak *Sq* current (30°–75° GLon) with our IHFACs in Figure 3c, we do not find the expected northern winter but more the summer configuration. A similarly contrasting IHFAC configuration is found in the sector of strong northern *Sq* currents (285°–300° GLon). Here we report southward currents around noon, as expected for a dominant *Sq* vortex in the southern hemisphere. Currently, we cannot explain the contrasting intensities between the *Sq* current system and the low-latitude IHFACs during northern winter.

5.1. Tidal Modulation of IHFACs

The IHFAC distribution presented in Figure 3 shows prominent longitudinal variations of intensity. For the June and equinox seasons the well-known longitudinal wave number-4 (WN-4) patterns are visible. Their role in IHFACs has earlier been studied by Park et al. (2011), and they are related to the nonmigrating diurnal DE3 tide propagating upward from the troposphere. Interestingly, Chulliat et al. (2016) report that these tidal waves mainly influence the southern *Sq* system, and they are hardly discernible in the northern hemisphere.

Quite different longitudinal IHFAC patterns are found during northern winter months. They suggest more the presence of a wave-1 tide, the nonmigrating semidiurnal SW1. Dashed and solid lines in Figure 3c mark possible locations of the phase fronts for the wave crest and trough, respectively. Park et al. (2011) already mentioned a similar tidal modulation of the December solstice IHFAC distribution. They suggested the nonmigrating terdiurnal tide TW2, which also causes a WN-1 pattern, but its phase slope is a little shallower (SW1 passes the 360° in longitude within 12 local time hour and TW2 in 8 LT hours). The small difference in slope may well lie within the range of uncertainty. Since the semidiurnal tide is more dominant in the atmosphere than the terdiurnal, we suggest it to be the more likely cause. Chulliat et al. (2016) report a strong WN-1 modulation of the *Sq* intensity in the northern hemisphere during winter. An interaction of it with the semidiurnal atmospheric tide can well cause the SW1. All this infers that the December IHFAC tidal patterns are mainly driven by northern hemisphere *Sq* dynamics.

The presentation of the IHFAC distribution in a local time versus longitude frame is well suited for identifying solar tides. However, the effects of other oscillations, that is, propagating planetary waves or lunar tides, are not visible in that frame. It is well known that semidiurnal lunar tidal signatures, that is, M2, are strongly enhanced in ionospheric quantities during times of stratospheric sudden warming (SSW) events (see the review by Chau et al., 2012). These SSW events lasting several weeks occur commonly during the months of January and February in the northern polar region. So far there are no reports about the lunar tidal modulation of IHFACs.

During the years taken into account in our study five SSW events occurred. Table 1 lists the dates and characters of those SSWs. Considering the amplifying effect of SSW on lunar tides we selected for our analysis the 93 days following 21 December of the years, which contained SSWs (starting 21 December 2014, ending 23 March 2019). For visualizing a possible tidal signature, the IHFAC density distribution is shown in Figure 9

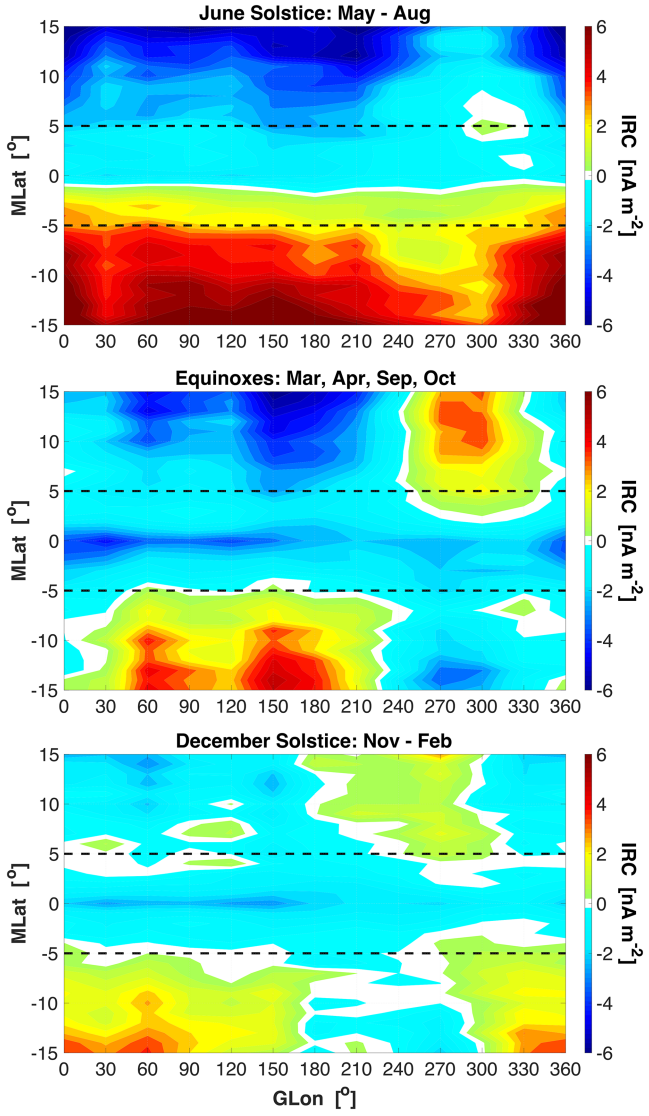

Figure 7. Magnetic latitude versus longitude distribution of radial *F* region currents in the noon sector separately for the three Lloyd seasons. Positive values represent upward flowing currents.

in a local time versus lunar phase frame. The lunar age is divided into 24 hr (Moon Phase) with 0 hr marking new moon epoch and 12 hr full moon. The IHFAC values are sorted into bins of 1 hr of local time by 1 hr of moon phase but smoothed over 2 hr in both directions.

In Figure 9 one can identify the modulation of IHFAC intensities by the lunar M2 tide. In order to derive quantitative results, we fitted an M2 tidal model to the observations. As a result, we obtain for the tidal amplitude 0.74 nA/m^{-2} and for the phase 4.7 hr. This means that the tidal crest appears at 4.7 MLT at new moon and full moon epochs. Solid lines in Figure 9 mark the derived tidal crest locations. For comparison, Lühr et al. (2012) report the M2 tidal crest appearance at 8.2 MLT for the equatorial electrojet during new and full moon epochs.

The derived mean M2 tidal amplitude is relatively small. However, our analysis interval of 93 days is about 3 times longer than the typical enhancement of the lunar tide during SSW events. When considering the effect of the long interval we may assume an SSW-related lunar tide enhanced to about 2.5 nA m^{-2}. This amounts to nearly half the peak amplitudes shown in Figures 3 and 9 for December solstice conditions; thus, it can be considered as an important contribution.

Figure 9 reveals for most of the moon phase hours the expected northern winter IHFAC polarity, negative around noon and positive in the morning and evening, although with rather low current densities. However, noontime current appears during the first half of the lunar cycle about 2 hr earlier than during the second. This may be caused by an interaction of the quasi-16-day planetary wave with the lunar tide. Only by sorting the northern winter IHFAC observations with respect to moon phase we come close to the expected interhemispheric current distribution.

In a recent paper He and Chau (2019) reported about wind measurements in the middle-latitude upper mesosphere derived by five radars. This setup allowed them to distinguish between temporal and spatial variations. They claim that the quasi-16-day planetary wave and the lunar tide are both enhanced during SSW events. By making use of multiple ground stations observations they can show that the interaction of the 16-day wave with the semidiurnal migrating solar tide can mimic the presence of the nonmigrating SW1. In Figure 3, bottom frame, we find SW1 signatures in the IHFAC distribution during northern winter months when SSWs occur frequently. This raises the question: is our highlighted SW1 tidal signal just a result of the interaction between planetary wave and tidal variation or does the SW1 really modulate the IHFACs? It would require simultaneous IHFAC observation at different longitudes (about 90° separated) to resolve the ambiguity.

5.2. Characteristics of Equatorial *F* Region Dynamo Currents

At latitudes close to the magnetic equator, below ±15° MLat, we have presented radial current density rather than FACs. From Figure 5, however, it is evident that IHFACs are typically sensed by Swarm A and C (at 460-km altitude) until ±5° MLat. By mapping down from this latitude along the field lines to the *E* region the footprint of the low-latitude IHFAC boundary reaches ±14° MLat. Hence, low-latitude IHFACs extend a little closer to the equator than ±20° MLat where we stopped the averaging in the above section.

At lower latitudes the wind-driven *F* region dynamo currents dominate. During daytime downward currents are prevailing above the equator and in the evening sector upward IRCs are flowing (see Figure 5). The intensity of derived IRCs varies from season to season. They are weakest during the months around June solstice. There are several quantities that can influence the *F* region dynamo strength. According to Park, Lühr, Fejer, and Min (2010) the radial sheet current density J_F can be expressed as

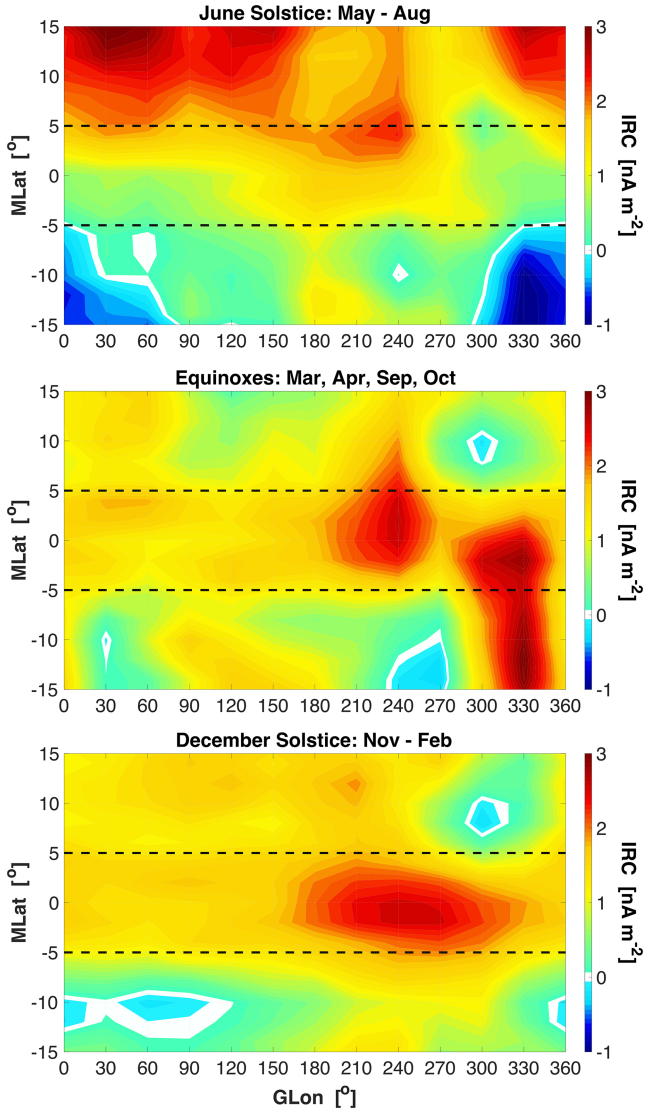

Figure 8. Same format as Figure 7 but for radial currents in the evening sector.

$$J_F = \frac{2\Sigma_P^E \Sigma_P^F}{2\Sigma_P^E + \Sigma_P^F} uB. \quad (2)$$

where $\Sigma^E{}_P$ ($\Sigma^F{}_P$) are the Pedersen integrated conductivities in the E (F) region, u is the zonal wind velocity, and B is the ambient horizontal field strength. During daytime $\Sigma^E{}_P$ is much larger than $\Sigma^F{}_P$; therefore, it is mainly the field-line integrated Pedersen conductivity in the F region that controls the vertical current intensity. Prime contributor to the conductivity is the electron density in the related fluxtube. The direction of currents is determined by the zonal wind, westward winds drive downward currents, and eastward wind cause upward currents. Thermospheric wind velocities depend only little on altitude. The horizontal magnetic field strength near the equator varies considerably with longitude, but part of that effect is compensated by the influence of the geomagnetic field on the Pedersen conductivity.

We observe weakest IRC values around June solstice months. This may to some extent be caused by weaker daytime zonal winds in that season and strongest during equinoxes, according to the horizontal wind model, HWM14. Here we bring, however, another aspect into consideration that is the altitude at which Swarm satellites pass the dynamo region. It is expected that the dynamo is most efficient in the fluxtube that includes the equatorial ionization anomaly (EIA) because of the enhanced conductivity. The apex altitude of the EIA depends strongly on the vertical plasma drift over the magnetic equator. Fejer et al. (2008) deduced the lowest noontime plasma drift velocities for the months May through August from ROCSAT-1 measurements, ranging around 15–20 m/s (see their Figure 4). Highest daytime vertical drifts are recorded during equinox seasons. This is consistent with the interpretation of crossing the daytime dynamo region at the very top part around June and more in the center part during equinoxes. The small IRC readings from June months are therefore caused by a combination of a weak F region dynamo and an unfavorable measurement height. The CHAMP orbits, at altitudes between 300 and 400 km, were better suited for sensing the daytime F region currents (Park, Lühr, & Min, 2010).

We observe also a systematic dependence of IRC intensity on longitude (see Figure 7). Equatorial current densities are larger in the eastern than in the western hemisphere. Following our line of arguments this means that the dynamo region reaches higher in the eastern part and is thus more favorable for Swarm measurements. This hemispheric difference is found in all seasons. Therefore, it seems to be an effect caused by the geomagnetic field geometry.

Also for the radial currents in the evening sector, we had a look at the longitudinal distribution. Compared to the other seasons the IRC density is again lowest around June solstice. But during the hours around sunset the EIA is expected to reach significantly higher altitudes. In the eastern hemisphere there appears a bifurcation of the radial current, best visible during equinox months but present also in other seasons (see Figure 8). We interpret this observation as a result of passing the duskside meridional current system below the dynamo region (see the cartoon in Figure 6). In the western hemisphere, centered around 240° GLon, strongest IRCs are found at all seasons. This is indicative of passing right through the dynamo region. It implies that the evening sector EIA is also lower in the western than in eastern hemisphere, the same tendency as deduced for the hours around noon.

Table 1
Dates of Stratospheric Sudden Warming Events During Our Study Period

SSW day vortex weakening	Classification
05/01/2015	Displaced
06/03/2016	Split
02/02/2017	Displaced
14/02/2018	Split
01/01/2019	Split

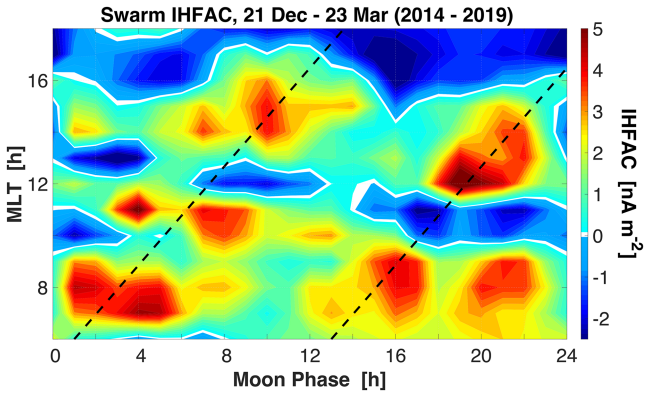

Figure 9. Lunar tidal modulation of IHFACs during SSW seasons. Dashed lines mark the locations of lunar M2 tidal crests.

Already the initial study (Lühr et al., 2015) reported more intense noontime equatorial IRC in the eastern hemisphere than in the western. They assumed the lower solar zenith angle in the eastern hemisphere, where the magnetic equator lies in the northern hemisphere, during the summer-dominated study interval as cause for stronger currents. This more comprehensive study disproves that assumption since the same longitude distribution of vertical current strength is found at December solstice. Equally with the evening IRC distribution, Lühr et al. (2015) found also the largest current strengths in the western hemisphere around 240° GLon (see their Figure 5). Their explanation was based on the alignment of the day-night terminator with the magnetic meridian in that longitude sector around June solstice. But we find peak current densities in the same sector also during December months. Therefore, their season-dependent argument cannot be correct. Our explanation of the obtained equatorial IRC intensity by the varying height of the *F* region dynamo region with respect to the Swarm orbit does not suffer such inconsistencies.

During the considered five-year period the orbit of Swarm A/C decayed from 475 to 445 km. This 30-km lowering is partly compensated by the expected altitude reduction of the *F* region peak height, as a result of the declining solar activity during the observation period. Therefore, we think that the orbital altitude changes will not have a big impact on our inferences.

5.3. Influence of the South Atlantic Anomaly

In all the plots showing the longitudinal variation of IHFAC densities the influence of the SAA is visible within the longitude range 300°–330° GLon. For example, in Figure 7 there is a reduced northward current around June solstice and an intense southward current during equinoxes. Similarly, prominent northward IHFACs in that area are observed in the evening (Figure 8) during equinox and December seasons. All this suggests that the *Sq* system is enhanced in the SAA region. It is suggested that a weak *B* field (lower ion gyrofrequency) shifts the effective dynamo altitude upward where the plasma density and wind speed are higher (Takeda, 1996). Hence, *Sq* currents near the SAA are expected to be stronger (more summer-like) than in the conjugate northern hemisphere during most seasons. Second, the *E* region conductivity may be enhanced in the SAA due to particle precipitation (e.g., Abdu et al., 2005). All these effects can contribute to current enhancements (summer-like *Sq* condition) around the SAA region.

5.4. Uncertainty Estimates of IHFAC and IRC

The presented average distributions of IHFACs and IRCs have partly small amplitudes, in the range of a few nA/m^2. Therefore, it may be worth assessing the reliability of the current estimates. The main error source for the dual-SC FAC estimates are differences in sensitivity between the magnetometers on Swarm A and C. Of particular relevance is the northward, *x* component. Near the magnetic equator, the *x* component is well represented by the total field, which is reliably measured by the scalar helium vapor magnetometers. Differences in the total field between the two spacecraft have been shown to be less than 0.5 nT. This amounts to an error of about 2.5 nA/m^2 in radial current when following the calculation by Ritter et al. (2013). Toward higher latitudes, the *x* component is influenced more and more by the measurements of the fluxgates and the uncertainties of the attitude. Here is a difference between spacecraft of 1 nT more typical. For our IHFAC data we better assume an uncertainty of 5 nA/m^2. However, these errors do not always have the same sign. Therefore, the resolution of the averages presented here is significantly higher than the error values calculated. The derived and presented current configuration can thus be considered reliable to a level of about 1 nA/m^2.

6. Summary

We presented comprehensive statistical investigations of low-latitude (14°–35° MLat) interhemispheric field-aligned currents and equatorial radial currents based on advanced Swarm multisatellite current estimates. Considering five years of measurements allows to resolve independently seasonal and local time

variations. Our results confirm several of the earlier reported observations of IHFACs, but other features appear during the months around December. Important findings can be summarized as follows:

1. During northern summer and fall equinox low-latitude FACs flow around noontime from the southern to the northern hemisphere, and FACs in the opposite direction flow in the morning and evening. This is largely consistent with the classical prediction, that is, by Fukushima (1979). This pattern of diurnal variation can be observed at almost all longitudes.
2. Conversely, unexpectedly lower and less well-structured mean IHFACs are observed during the months around December and early spring. There are significant variations in FAC intensity and direction depending on longitude. These suggest the modulation of IHFACs by the solar semidiurnal tide SW1. In addition, we find a modulation of current strength by the lunar M2 tide when analyzing periods around stratospheric sudden warming events. All these atmospheric waves and tides are probably responsible for the complicated IHFAC patterns during northern winter.
3. We can confirm the presence of vertical currents above the magnetic equator, flowing downward around noon and upward in the evening. Their intensity is weakest around June solstice and strongest during equinoxes. Peak current densities are observed around June solstice about 1 hr earlier than during the rest of the year.
4. The lower Swarm satellite pair (at ~460-km altitude) crosses the noontime *F* region dynamo at its upper part or slightly above. This can be deduced from the observations of the field-aligned currents connected to the topside of the dynamo region. Therefore, only weak downward current densities are recorded, in particular at western longitudes where the dynamo center is lower than at eastern longitudes.
5. Radially upward currents in the evening sector appear to be stronger. This is interpreted as a more favorable crossing of the dynamo region, which is higher around that time. Observations imply the same altitude variation with longitude as for noontime. Largest current recordings around 240° longitude suggest an optimal crossing height, while weaker readings in the eastern hemisphere imply sampling at the lower part of the dynamo region.
6. A region outstanding in the current distribution is the longitude sector containing the South Atlantic Anomaly. We suggest that the enhanced ionospheric conductivity, due to the reduced magnetic field strength and other effects, resembles summer conditions through all seasons of the year.

The presented observations have revealed a number of unexpected *F* region low-latitude current features. These are worth to be studied in more details. In particular, dedicated numerical modeling could help to identify the processes involved.

Acknowledgments
We thank Jaeheung Park for the fruitful scientific discussion about low-latitude Swarm radial currents and Yunliang Zhou for helping with the lunar tidal analysis. The European Space Agency (ESA) is acknowledged for providing the Swarm data and for financially supporting the work of developing the Level-2, CAT-2 products. The data used here are the Swarm Level-2 product FAC (FAC_TMS_2F) that is freely accessible to all users via ftp://swarm-diss.eo.esa.int/Level2daily/Latest_baselines/FAC/TMS/Sat_AC/ and includes both FAC and IRC. G.K. and C.S. were partially supported by the ESA project "VERA" (contract 4000126709/19/NL/IA).

References

Abdu, M. A., Batista, I. S., Carrasco, A. J., & Brum, C. G. M. (2005). South Atlantic magnetic anomaly ionization: A review and a new focus on electrodynamic effects in the equatorial ionosphere. *Journal of Atmospheric and Solar - Terrestrial Physics*, *67*(17-18), 1643–1657. https://doi.org/10.1016/j.jastp.2005.01.014

Bolaji, O. S., Rabiu, A. B., Oyeyemi, E. O., & Yumoto, K. (2012). Climatology of the inter-hemispheric field-aligned currents system over the Nigeria ionosphere. *Journal of Atmospheric and Solar-Terrestrial Physics*, *89*, 144–153. https://doi.org/10.1016/j.jastp.2012.07.008

Campbell, W. H. (1989). The regular geomagnetic field variations during quiet solar conditions. In J. A. Jacobs (Ed.), *Geomagnetism* (Vol. 3, pp. 385–460). New York: Academic Press.

Chau, J. L., Goncharenko, L. P., Fejer, B. G., & Liu, H.-L. (2012). Equatorial and low latitude ionospheric effects during sudden stratospheric warming events. *Space Science Reviews*, *168*(1–4), 385–417. https://doi.org/10.1007/s11214-011-9797-5

Chulliat, A., Vigneron, P., & Hulot, G. (2016). First results from the swarm dedicated ionospheric field inversion chain. *Earth, Planets and Space*, *68*(1), 1–18. https://doi.org/10.1186/s40623-016-0481-6

Fathy, A., Ghamry, E., & Arora, K. (2019). Mid and low-latitudinal ionospheric field-aligned currents derived from the swarm satellite constellation and their variations with local time, longitude, and season. *Advances in Space Research*, *64*(8), 1600–1614. https://doi.org/10.1016/j.asr.2019.07.022

Fejer, B. G., Jensen, J. W., & Su, S.-Y. (2008). Quiet time equatorial *F* region vertical plasma drift model derived from ROCSAT-1 observations. *Journal of Geophysical Research*, *113*(A5), A05304. https://doi.org/10.1029/2007JA012801

Friis-Christensen, E., Lühr, H., Knudsen, D., & Haagmans, R. (2008). Swar: An earth observation Mission investigating Geospace. *Advances in Space Research*, *41*(1), 210–216. https://doi.org/10.1016/j.asr.2006.10.008

Fukushima, N. (1979). Electric potential difference between conjugate points in middle latitudes caused by asymmetric dynamo in the ionosphere. *Journal of Geomagnetism and Geoelectricity*, *31*(3), 401–409. https://doi.org/10.5636/jgg.31.401

Fukushima, N. (1994). Some topics and historical episodes in geomagnetism and aeronomy. *Journal of Geophysical Research*, *99*(A10), 19,113–19,142. https://doi.org/10.1029/94JA00102

He, M., & Chau, J. L. (2019). Mesospheric semidiurnal tides and near-12 h waves through jointly analyzing observations of five specular meteor radars from three longitudinal sectors at boreal midlatitudes. *Atmospheric Chemistry and Physics*, *19*(9), 5993–6006. https://doi.org/10.5194/acp-19-5993-2019

Lühr, H., Kervalishvili, G., Michaelis, I., Rauberg, J., Ritter, P., Park, J., et al. (2015). The inter-hemispheric and *F*-region dynamo currents revisited with the swarm constellation. *Geophysical Research Letters*, *42*, 3069–3075. https://doi.org/10.1002/2015GL063662

Lühr, H., & Maus, S. (2006). Direct observation of the *F* region dynamo currents and the spatial structure of the EEJ by CHAMP. *Geophysical Research Letters*, *33*, L24102. https://doi.org/10.1029/2006GL028374

Lühr, H., Park, J., Ritter, P., & Liu, H. (2012). In-situ CHAMP observation of ionosphere-thermosphere coupling. *Space Science Reviews*, *168*(1-4), 237–260. https://doi.org/10.1007/s11214-011-9798-4

Lühr, H., Ritter, P., Kervalishvili, G., & Rauberg, J. (2020). Applying the dual-spacecraft approach to the swarm constellation for deriving radial current density. In M. W. Dunlop & H. Lühr (Eds.), *Ionospheric Multi-Spacecraft Analysis Tools*, *ISSI Scientific Report Series 17* (pp. 117–140). Switzerland: Springer Nature. https://doi.org/10.1007/978-3-030-26732-2_6

Maeda, H. (1974). Field-aligned current induced by asymmetric dynamo action in the ionosphere. *Journal of Atmospheric and Terrestrial Physics*, *36*(8), 1395–1401. https://doi.org/10.1016/0021-9169(74)90216-5

Maeda, H., Iyemori, T., Araki, T., & Kamei, T. (1982). New evidence of a meridional current system in the equatorial ionosphere. *Geophysical Research Letters*, *9*(4), 337–340.

Olsen, N. (1997). Ionospheric *F* region currents at middle and low latitudes estimated from Magsat data. *Journal of Geophysical Research*, *102*(A3), 4563–4576. https://doi.org/10.1029/96JA02949

Owolabi, O. P., Bolaji, O. S., Adeniyi, J. O., Oyeyemi, E. O., Rabiu, A. B., & Habarulema, J. B. (2018). Excursions of interhemispheric field-aligned currents in Africa. *Journal of Geophysical Research: Space Physics*, *123*(7), 6042–6053. https://doi.org/10.1029/2017JA025083

Park, J., Lühr, H., Fejer, B. G., & Min, K. W. (2010). Duskside *F*-region dynamo currents: Its relationship with prereversal enhancement of vertical plasma drift. *Annales de Geophysique*, *28*(11), 2097–2101. www.ann-geophys.net/28/2097/2010/, https://doi.org/10.5194/angeo-28-2097-2010

Park, J., Lühr, H., & Min, K. W. (2010). Characteristics of *F*-region dynamo currents deduced from CHAMP magnetic field measurements. *Journal of Geophysical Research*, *115*(A10), A10302. https://doi.org/10.1029/2010JA015604

Park, J., Lühr, H., & Min, K. W. (2011). Climatology of the inter-hemispheric field-aligned current system in the equatorial ionosphere as observed by CHAMP. *Annales de Geophysique*, *29*(3), 573–582. https://doi.org/10.5194/angeo-29-573-2011

Rishbeth, H. (1971). The *F*-layer dynamo. *Planetary and Space Science*, *19*(2), 263–267. https://doi.org/10.1016/0032-0633(71)90205-4

Ritter, P., Lühr, H., & Rauberg, J. (2013). Determining field-aligned currents with the swarm constellation mission. *Earth, Planets and Space*, *65*(11), 1285–1294. https://doi.org/10.5047/eps.2013.09.006

Shinbori, A., Koyama, Y., Nosé, M., Hori, T., & Otsuka, Y. (2017). Characteristics of seasonal variation and solar activity dependence of the geomagnetic solar quiet daily variation. *Journal of Geophysical Research: Space Physics*, *122*, 10,796–10,810. https://doi.org/10.1002/2017JA024342

van Sabben, D. (1964). North-south asymmetry of *Sq*. *Journal of Atmospheric and Terrestrial Physics*, *26*(12), 1187–1195. https://doi.org/10.1016/0021-9169(64)90127-8

van Sabben, D. (1966). Magnetospheric currents, associated with the N-S asymmetry of *Sq*. *Journal of Atmospheric and Terrestrial Physics*, *28*(10), 965–982. https://doi.org/10.1016/S0021-9169(17)30026-0

Takeda, M. (1996). Effects of the strength of the geomagnetic main field strength on the dynamo action in the ionosphere. *Journal of Geophysical Research*, *101*(A4), 7875–7880. https://doi.org/10.1029/95JA03807

Takeda, M., & Maeda, H. (1983). *F*-region dynamo in the evening. Interpretation of equatorial *D* anomaly found by Magsat. *Journal of Atmospheric and Terrestrial Physics*, *45*(6), 401–408. https://doi.org/10.1016/S0021-9169(83)81099-X

Yamashita, S., & Iyemori, T. (2002). Seasonal and local time dependences of the interhemispheric field-aligned currents deduced from the Ørsted satellite and the ground geomagnetic observations. *Journal of Geophysical Research*, *107*(A11), 1372. https://doi.org/10.1029/2002JA009414

Yamazaki, Y., & Maute, A. (2017). *Sq* and EEJ—A review on the daily variation of the geomagnetic field caused by ionospheric dynamo currents. *Space Science Reviews*, *206*(1–4), 299–405. https://doi.org/10.1007/s11214-016-0282-z